Quantum and disorder effects in Davydov soliton theory

Wolfgang Förner
Institut für Physikalische und Theoretische Chemie and Laboratory of the National Foundation for Cancer Research, Universität Erlangen-Nürnberg, Egerlandstrasse 3, D-8520 Erlangen, Germany
(Received 3 December 1990)

Within the simple displaced oscillator state ansatz of Davydov [Phys. Scr. **20**, 387 (1979)], called the D_2 ansatz state, the soliton remains stable against strong disorder in the sequences of masses, spring constants, and coupling constants. However, weak diagonal disorder or disorder in the dipole coupling constants destroys the solitons. Within the D_1 ansatz, in which the quantum nature of the lattice plays a greater role than in the classical D_2 state, the soliton appears only from nonlinearities roughly 3 to 4 times larger than those in D_2 models. The sensitivity of such solitons to disorder is practically opposite that for the D_2 state. Within the partial dressing model we find only dispersing solitary waves, no real traveling solitons. The sensitivity of such waves to disorder is similar to the D_1 case.

I. INTRODUCTION

For the explanation of a wide variety of chemical and physical phenomena the introduction of nonlinear forces turned out to be necessary, e.g., a lattice bound by linear forces (harmonic) would have an infinite heat conductivity [1]. In a channel near Edinburgh a nondispersive localized wave packet was observed as the first example of a solitary wave [2]. Solitary solutions can only occur for nonlinear wave equations, since linear wave packets disperse rapidly. As some examples for an introduction of soliton concepts in physics and chemistry let us mention the dynamics of magnetic materials [3,4], rotations around carbon–carbon bonds in polyethylene [5], phase changes in solids [6,7], dynamics of the sugar-phosphate backbone [8] or the nucleotide bases [9] in DNA, and the spinless charge transport in *trans*- polyacetylene [10].

Many biological processes are associated with an energy transfer through proteins, where this energy is released by hydrolysis of adenosine triphosphate (ATP). The mechanism of this energy transport is not quite clear [11]. As an alternative to electronic mechanisms [11] one can assume that the energy is stored as vibrational energy in the amide-I mode (CO stretch) of a polypeptide chain. Following Davydov's idea [12] one can take into account the coupling between the amide-I vibration and the acoustic phonons of the lattice. Through this coupling nonlinear terms appear in the equations of motion. In this way the energy can be transported in solitary waves. Direct experimental evidence for the existence of such solitons in proteins is still lacking. This is due to the complex structure of proteins, which makes such measurements very difficult. However, in acetanilide crystals a substructure with chains of hydrogen bonds similar to proteins is present. In low-temperature infrared and Raman spectra of this material a new band in the amide-I region appears. Up to now this band could only be explained with the help of a model similar to the Davydov soliton concept in proteins [13]. In this case the CO oscillators are coupled to optical phonons and the soliton would be pinned. Recent experiments, however, suggest a conventional mode strongly coupled to the phonons to be responsible for the observed new band [14].

A very important feature of most nonlinear systems, especially proteins, is disorder. However, this problem is seldom discussed in the field of soliton dynamics. It was done numerically for solitons in *trans*-polyactylene [10] by several groups, for classical molecular dynamics of peptide units moving in a Lennard-Jones potential [15], and in model potentials of cubic and quartic nature [16], for example. For Davydov solitons in the displaced oscillator state ansatz (D_2 ansatz) we have performed such a study [17–19]. Also in a model for a stacked system we have considered impurity molecules [20]. However, there exist more sophisticated ansatz states than D_2 for Davydov solitons, in which the quantum nature of the lattice is more pronounced. Thus after a short review of our previous results on D_2 dynamics we want to focus mainly on disorder effects in the more sophisticated models.

II. THE D_2 ANSATZ STATE: A SHORT REVIEW

The Hamiltonian used for this study is in the most simple form for the system investigated by Davydov [12]; however, it is extended for the possibility of disorder. Disorder is present in any protein due to the 20 natural amino acids which form proteins. More sophisticated forms of the Hamiltonian which incorporate more details of the protein structure have led qualitatively to the same results [21]:

$$\hat{H}=\sum_n \Big[(E_0+E_n)\hat{a}_n^\dagger\hat{a}_n - J_n(\hat{a}_n^\dagger\hat{a}_{n+1}+\hat{a}_{n+1}^\dagger\hat{a}_n) + \frac{\hat{p}_n^2}{2M_n} + \tfrac{1}{2}W_n(\hat{q}_n-\hat{q}_{n-1})^2 + X_n\hat{a}_n^\dagger\hat{a}_n(\hat{q}_n-\hat{q}_{n-1}) \Big] . \quad (1)$$

In (1) $\hat{a}_n^\dagger$ ($\hat{a}_n$) are the usual boson creation (annihilation) operators [22] for the amide-I oscillators at sites n (see Fig. 1). From infrared spectra the excitation energy of an

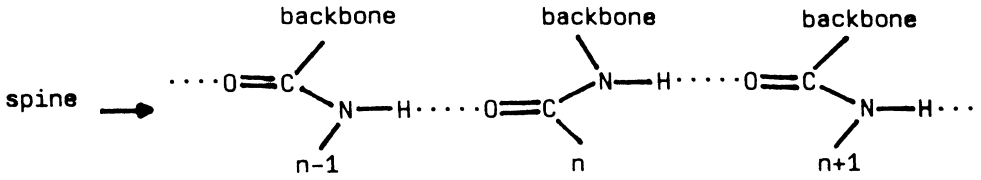

FIG. 1. Schematic picture of a hydrogen bonded channel (spine) in a protein helix (indicated by backbone, perpendicular to the spine).

isolated amide-I oscillator can be deduced to $E_0=0.205$ eV [23]. E_n stands for the diagonal disorder. Usually for all parameters in (1) site-independent mean values are used. The average value of the dipole-dipole coupling between neighboring amide-I oscillators is $J=0.967$ meV [23]. The average spring constant of the hydrogen bonds is taken usually to be $W=13$ N/m [23]. $\hat{p}_n$ is the momentum and $\hat{q}_n$ the position operator of unit n. The average mass M is taken as that of myosine ($M=114m_p$; m_p is a proton mass) [23]. The energy of the CO stretch in hydrogen bonds is a function of the length R of the hydrogen bond ($E=E_0+XR$) [24]. For X the experimental value is 62 pN [24]. *Ab initio* calculations on formamide dimers usually lead to $X=30-50$ pN [25].

For the solution of the time-dependent Schrödinger equation

$$\hat{H}|\psi\rangle=i\hbar\frac{\partial}{\partial t}|\psi\rangle \tag{2}$$

we use the displaced oscillator state ansatz of Davydov [12], the so-called D_2 ansatz.

In the displaced oscillator state ansatz $q_n(t)$ is the expectation value of the position operator, $p_n(t)$ is that of the momentum operator of site n, $|0\rangle$ is the vacuum state, and $|a_n'(t)|^2$ is the probability of finding an amide-I vibrational quantum at site n, provided that $\sum_n|a_n'(t)|^2=1$.

$$|\psi\rangle=\sum_n a_n'(t)\hat{a}_n^{\dagger}\exp[-\hat{S}(t)]|0\rangle\ , \tag{3a}$$

$$\hat{S}(t)=\frac{i}{\hbar}\sum_m[\hat{p}_m q_m(t)-\hat{q}_m p_m(t)]\ . \tag{3b}$$

The equations of motion can be derived either by using the expectation value of $\hat{H}$ as the classical Hamiltonian function [12,21] or by quantum-mechanical methods [26]. After a gauge transformation one obtains

$$i\hbar\dot{a}_n=-(J_n a_{n+1}+J_{n-1}a_{n-1})+X_n(q_n-q_{n-1})a_n+E_n a_n\ , \tag{4a}$$

$$\dot{p}_n=W_{n+1}(q_{n+1}-q_n)-W_n(q_n-q_{n-1})+X_{n+1}|a_{n+1}|^2-X_n|a_n|^2\ , \tag{4b}$$

$$\dot{q}_n=\frac{p_n}{M_n};\quad a_n'=a_n\exp(-iE_0t/\hbar)\ . \tag{4c}$$

The complex equation (4a) was solved as a system of two coupled equations for the real and imaginary parts of a_n. The system of units eV for energy, Å for length, and ps for time proved to be suitable for a numerical solution of (4). For this purpose a fourth-order Runge-Kutta algorithm was used [27]. With a time step size of 0.01 ps in the simulations the total energy was conserved up to 3 μeV (0.015%). A possible imaginary part of the energy which can occur due to numerical inaccuracies was zero to an accuracy of 0.002 feV. The norm was conserved up to 0.4 ppm (parts per million). Note that we used fixed chain ends and as an initial excitation we put one quantum at the site $N-1$, where N is the number of units chosen to be $N=200$ in our simulations. For the lattice $q_n(0)=p_n(0)=0$ was applied.

For the sake of comparison we show in Fig. 2 a survey of the (X,W) parameter space for the D_2 ansatz using ordered chains and in Fig. 3 a series of dynamics using standard parameters in ordered chains but different values of X [19]. For $X=20$ pN (3a) the system is dispersive; for $X=60$ pN (3b) a traveling soliton appears. This holds between 40 and 80 pN for X [21]. For $X=100$ pN (3c) the soliton is pinned.

Turning to disorder we review shortly the results of Refs. [18] and [19]. To introduce disorder we have used a random number generator to create random sequences of the different parameters along the chain. Disorder in the mass sequence destroys the soliton only for a very large disorder strength, with M_n values $0.01M<M_n<50M$ [17]. For $0.01M<M_n<10M$ the soliton velocity is reduced from 0.73 to 0.59 km/s, the sound velocity to 2.12 km/s. In the case of the mass variation of natural amino

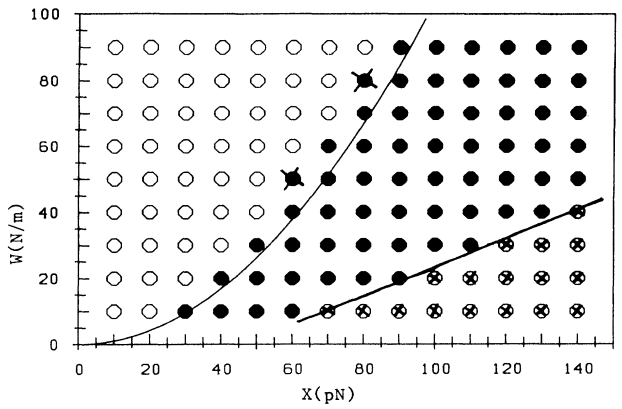

FIG. 2. A survey of the (X,W) parameter space in D_2 dynamics for standard parameters otherwise. Each circle represents a simulation (○, dispersive; ◙, slowly dispersive traveling solitary wave; ●, travelling soliton, ⊗, pinned soliton), the solid line gives the threshold for soliton formation in continuum theory.

acids ($0.66M < M_n < 1.79M$) virtually no change in the solitondynamics is found, thus the average-mass approximation is justified. In addition to modeling the natural degree of disorder in the masses, we have varied W_n. Up to a random variation of $\pm 20\% W$ we find no change in the dynamics. For $\pm 30\% W$ the soliton velocity is somewhat reduced to 0.68 km/s. Finally, for $\pm 40\% W$ the excitation disperses slowly and the propagation is irregular. For variations in J alone or together with the natural mass variation the soliton is stable up to $\pm 5\% J$. Thus the soliton is far more sensitive to variations in J_n than in the other parameters. If in addition W_n is aperiodic the

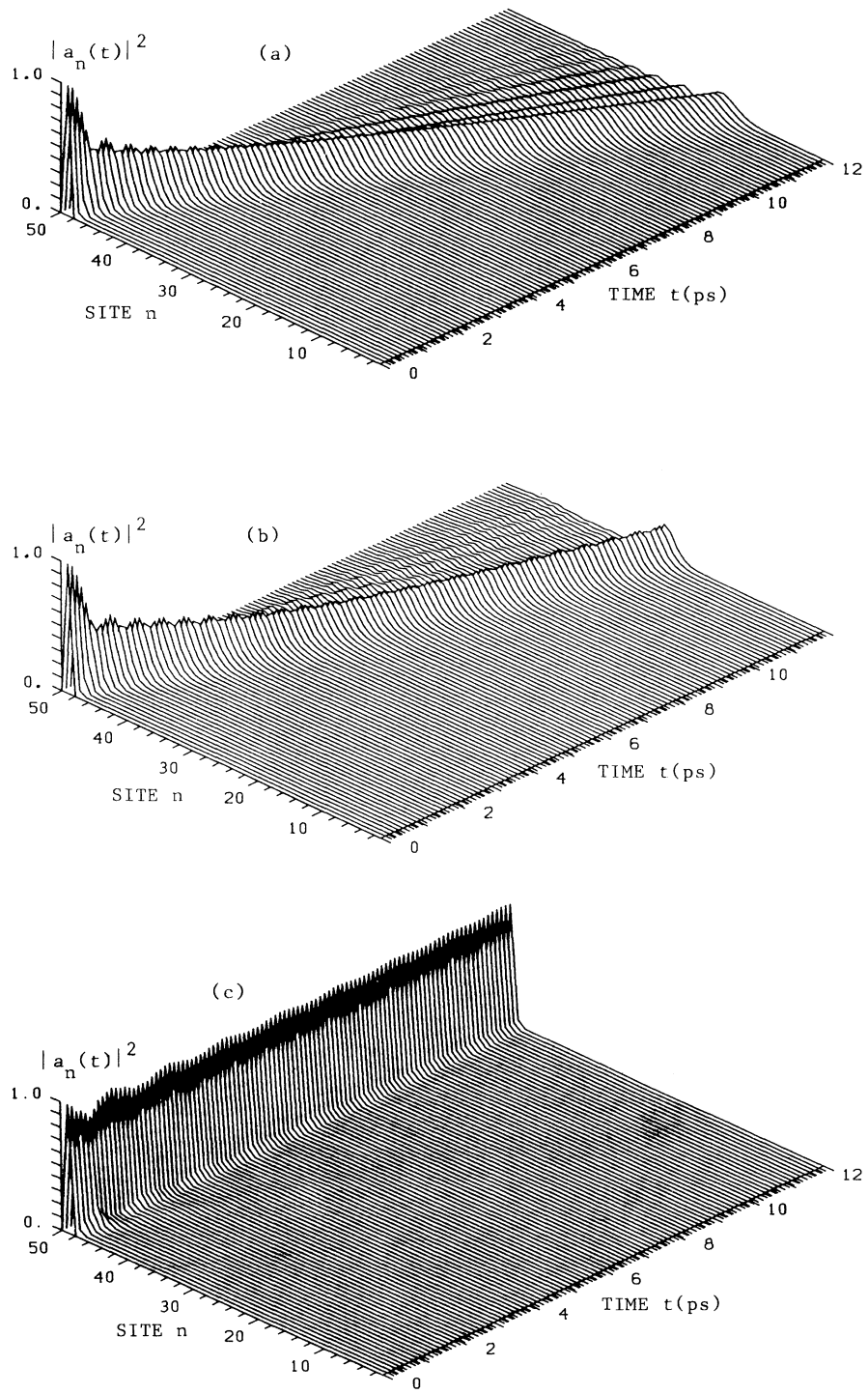

FIG. 3. Time evolution of $|a_n(t)|^2$ for the D_2 ansatz state using standard parameters with $X = 20$ pN (a), 60 pN (b), and 100 pN (c) in an ordered chain.

soliton is stable up to $\pm 10\% W$ while at $\pm 20\% W$ slowly dispersive behavior appears. Finally, if X_n alone is aperiodic, or if X_n is aperiodic together with the natural mass variation, X_n can be varied up to $\pm 20\% X$ without destruction of the soliton. However, if disorder in W_n is also introduced, X_n can be varied up to $\pm 15\% X$ and W_n up to $\pm 40\% W$. Finally if all four parameters are randomly varied the maximal possible disorder that would still allow the existence of a soliton is $\pm 20\% W$, $\pm 2.5\% J$, and $\pm 10\% X$. For this disorder strength we have calculated 10 different randomly chosen sequences to find out whether the soliton properties depend only on the magnitude of disorder or also on the individual sequences. We found that only the soliton velocity is affected; in this case it varies between 0.61 and 0.80 km/s.

In the case of diagonal disorder (E_n) [19] we found that for an isolated impurity in the middle of the chain ($E_n = E\delta_{n,100}$) the soliton can pass the impurity only if $E < 0.5$ meV. In other cases it is reflected or destroyed. In other cases it is reflected or destroyed. In the case of a random sequence ($E_n = E\beta_n$, $|\beta_n| \leq 1$, β_n random) only for $E < 1$ meV can the soliton pass the chain. For higher values of E the excitation disperses quickly.

However, the actual degree of disorder in proteins is unknown. The disorder in effective masses should be smaller than the mass interval of the natural amino acids since they are not free particles but are covalently bound in the main polypeptide chain. Disorder in the other parameters should be mainly due to small influences of the side groups on the geometry of the main chain. Thus one can conclude that the naturally occurring disorder in the parameters should be smaller than the maximal disorder in which the soliton is stable. Natural disorder may interfere with the soliton only when J_n and E_n are varied since the stability interval in these cases is rather small. We could not find any case where strong disorder stabilizes the soliton as reported in [16] for model systems.

III. THE D_1 ANSATZ STATE

In Appendix A we briefly derive the disordered Hamiltonian

$$\hat{H} = \sum_n \left[(E_0 + E_n)\hat{a}_n^\dagger \hat{a}_n - J_n(\hat{a}_{n+1}\hat{a}_n + \hat{a}_n^\dagger \hat{a}_{n+1}) + \sum_k \hbar\omega_k B_{nk}(\hat{b}_k + \hat{b}_k^\dagger)\hat{a}_n^\dagger \hat{a}_n \right] + \sum_k \hbar\omega_k \hat{b}_k^\dagger \hat{b}_k \ . \quad (5)$$

The matrix $\underline{B}$ is also given in Appendix A. The D_1 ansatz state as introduced by Davydov and also used to incorporate temperature effects [28] reads as

$$|D_1\rangle = \sum_n a_n'(t)\hat{a}_n^\dagger |0\rangle_{\text{ex}} |\beta_n(t)\rangle \quad (6)$$

with

$$|\beta_n(t)\rangle = \exp[-\hat{S}_n(t)]|0\rangle_{\text{ph}} = \exp\left[-\sum_k (b_{nk}^* \hat{b}_k - b_{nk}\hat{b}_k^\dagger) \right] |0\rangle_{\text{ph}} \ . \quad (7)$$

This ansatz allows dynamical phase mixing between phonons (ph) and excitons (ex). Thus the quantum nature of the lattice is more pronounced than in the D_2 ansatz. If one uses the expectation value of (6) with $\hat{H}$ as a classical Hamiltonian function one obtains equations of motion [28,29] which do not reproduce the exact solutions in the transportless case ($J = 0$) [30]. However, in contrast to D_2, for D_1 quantum-mechanical methods (QM's) give equations of motion that do reproduce the exact special case solutions [31,32]. In fact it was shown [32] that different QM's lead to the same equations. These are (Re and Im denote real and imaginary parts of their arguments, $\underline{B}$ is real as mentioned in Appendix A)

$$i\hbar\dot{a}_n = \left[E_n - \tfrac{1}{2} i\hbar \sum_k (\dot{b}_{nk} b_{nk}^* - \dot{b}_{nk}^* b_{nk}) + \sum_k \hbar\omega_k [2B_{nk}\,\text{Re}(b_{nk}) + |b_{nk}|^2] \right] a_n - J_n D_{n,n+1} a_{n+1} - J_{n-1} D_{n,n-1} a_{n-1} \ , \quad (8)$$

$$a_n'(t) = a_n(t)\exp(-iE_0 t/\hbar) \ , \quad (9)$$

$$D_{n,n'} = \exp\left[-\tfrac{1}{2} \sum_k [|b_{nk} - b_{n'k}|^2 + 2i\,\text{Im}(b_{n'k}^* b_{nk})] \right] \ , \quad (10)$$

$$i\hbar\dot{b}_{nk} = \hbar\omega_k(b_{nk} + B_{nk}) - J_n D_{n,n+1}(b_{n+1,k} - b_{nk})a_{n+1}/a_n - J_{n-1} D_{n,n-1}(b_{n-1,k} - b_{nk})a_{n-1}/a_n \ . \quad (11)$$

To avoid numerical difficulties due to the denominators $a_n(t)$ in (11) we use the same initial excitation as in [31]

$$a_n(0) = \left[1 - \sum_{n=1}^{N} |e_n|^2 (1 - \delta_{n,n_0}) \right]^{1/2} \delta_{n,n_0} + e_n(1 - \delta_{n,n_0}) \ , \quad (12)$$

where n_0 is the excitation site and $e_n = 0.005$ [31]. As in [19] we work with a Runge-Kutta method correct up to fourth order to solve (8) and (11) numerically. The momenta p_n of the units are (see Appendix A for definition of $\underline{U}$ and ω_k)

$$p_n = \sum_{k,n} (2\hbar M_n \omega_k)^{1/2} U_{nk} |a_m|^2 \,\text{Im}(b_{mk}) \ , \quad (13)$$

$$q_n = \sum_{k,m} (2\hbar / M_n \omega_k)^{1/2} U_{nk} |a_m|^2 \,\text{Re}(b_{mk}) \ . \quad (14)$$

The total energy is given by

$$E_t = \sum_n (E_0 + E_n)|a_n|^2 - \sum_n (J_n D_{n,n+1} a_n^* a_{n+1} + J_{n-1} D_{n,n-1} a_n^* a_{n-1}) + \sum_{n,k} \hbar\omega_k |a_n|^2 [|b_{nk}|^2 + 2B_{nk}\,\text{Re}(b_{nk})] \ . \quad (15)$$

In a typical run for $N = 50$, $n_0 = 49$ using as time step

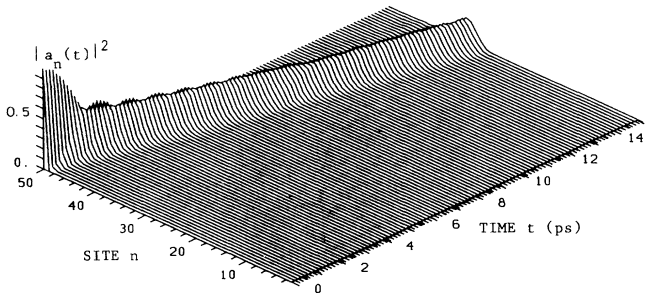

FIG. 4. Time evolution of $|a_n(t)|^2$ for the D_2 ansatz state as in [31] for $X=174$ pN (all conditions as in [31]).

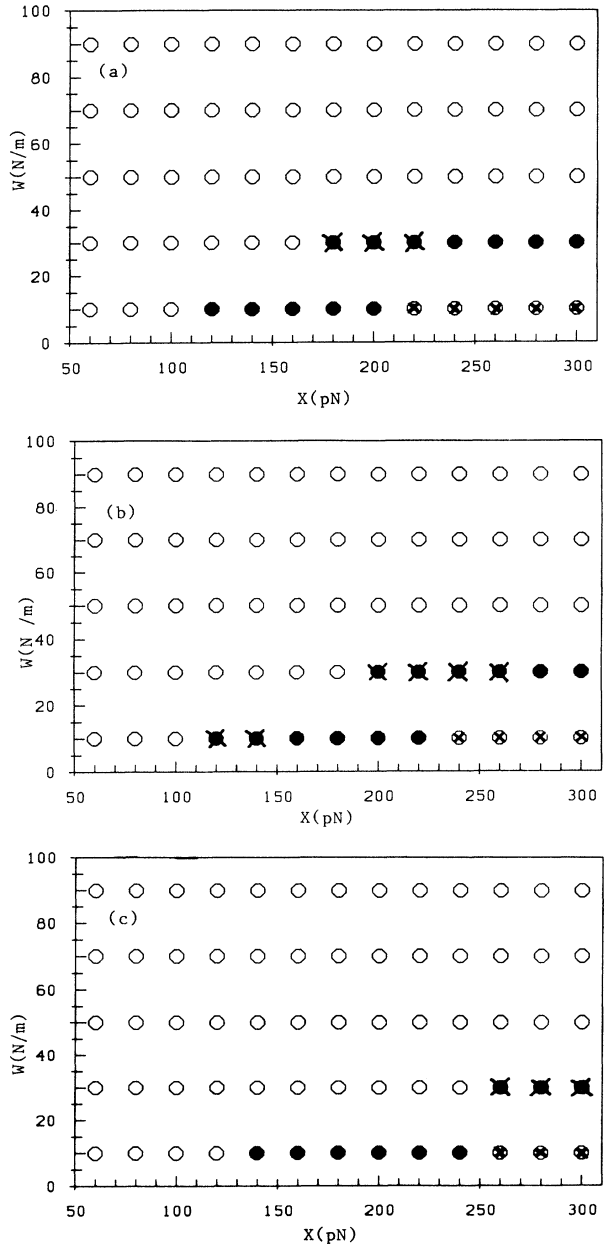

FIG. 5. Same as Fig. 2 for the D_1 state with $J=0.6$ meV (a), 1.0 meV (b), and 1.4 meV (c).

$\tau=0.01$ ps through 12 ps the error in E_t is less than 11 μeV ($\approx 0.005\% E_t$) and the norm is conserved up to 0.5 ppm. The translational mode ($\omega=0$) was not populated. To check our program we reproduced the results given in [31] where slightly different initial conditions and parameters were used. In Fig. 4 we show $|a_n(t)|^2$ for one of these runs.

Figure 5 shows our survey of the (X,W,J) parameter space for ordered chains. Obviously traveling solitons exist only for $W<50$ N/m independent of J in contrast to D_2 dynamics. Also the solitons occur for much larger values of X. The threshold value of X increases with increasing J or W. Obviously one cannot expect soliton formation below $X\approx 120$ pN in D_1 dynamics. This value is well above all estimates of X for proteins (≈ 30–60 pN). However, there exists an experimental estimate of X for the N–H vibration as large as 339 pN [33]. Moreover, Brown and Ivic [34] point out that the quantum nature of the lattice may well be overestimated in D_1. For comparison we show in Fig. 6 some examples of D_1 dynamics ($W=13$ N/m, $J=0.967$ meV). For $X=142$ pn [Fig. 6(a)] the excitation is still dispersive. Only at $X=174$ pN [Fig. 6(b)] is a traveling soliton obtained while between $X=200$ pN [Fig. 6(c)] and 280 pN [Fig. 6(d)] (in this case $W=10$ N/m was used) pinning occurs, in full agreement with [31]. The inclusion of temperature effects into D_1 theory is given in Appendix B.

Turning now to disorder we concentrate on a parameter set ($W=13$ N/m, $J=0.967$ meV, $X=180$ pN, $M=114m_p$) which allows traveling solitons. In Fig. 7(a) the time evolution of $|a_n|^2$ is shown where the masses have a random sequence between the lightest amino acid (glycine) and the heaviest (tryptophane). Obviously the soliton survives the mass disorder occurring in proteins. If the unit in the middle of the chain has a spring constant of $0.96W$ (or $1.04W$) the soliton is able to pass the impurity [Fig. 7(b)]. Only a small fraction of the excitation is reflected. For an impurity with $0.93W$ (or $1.07W$) most of the excitation is reflected in a dispersive manner and also the passing fraction broadens [Fig. 7(c)]. If the sequence of spring constants is random, already for a disorder of $\pm 2\% W$ [$W_n=(1+\beta_n)W$, $|\beta_n|\leq 0.02$, β_n random] [Fig. 7(d)] the soliton disperses slowly and is destroyed for $\pm 4\% W$ [Fig. 7(e)]. If in addition to a disorder of $\pm 2\% W$ the mass disorder is present the soliton disperses also. The situation for disorder in the nonlinearity (X) is similar. However, for an impurity of $0.93X$ in the middle of the chain [Fig.7(g)] the soliton disperses, while an additional mass disorder seems to stabilize the soliton somewhat in this case [Fig. 7(h)]. Up to an impurity strength of $0.98X$ the soliton is able to pass the impurity. Random disorder in X with or without mass disorder destroys the soliton starting with a disorder strength of $\pm 2\% X$.

Obviously the quantum nature of the lattice destabilizes the soliton considerably against disorder in X and W compared with the D_2 state. In the case of the dipole-dipole coupling J the soliton is more stable. With or without mass disorder it is able to override impurities up to $0.85J$ (for $1.15J$ the picture is identical). A random sequence in J causes a slow dispersion from $\pm 15\% J$ disor-

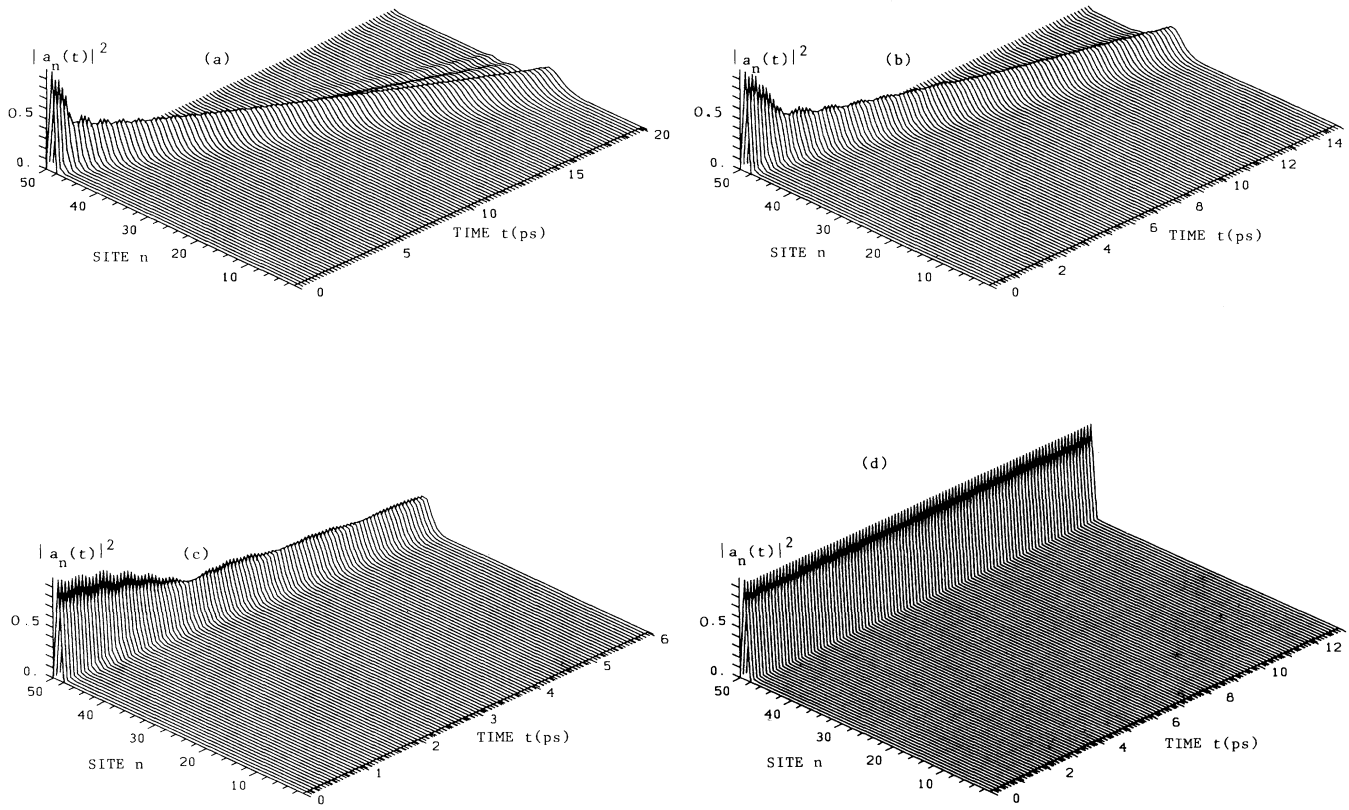

FIG. 6. Time evolution of $|a_n|^2$ for the D_1 state ($W=13$ N/m, $J=0.967$ meV) for $X=142$ pN (a), 174 pN (b), 200 pN (c), and 280 pN (d) (in this case $W=10$ N/m).

der strength. Additional mass disorder speeds up the dispersion of the wave. Also against diagonal disorder [E_n in Eq. (5)] the soliton is quite unstable. Up to an impurity strength of 0.3 meV in the middle of the chain the soliton overrides it, whether additional mass disorder is present or not. Random sequences $|E_n| \leq 0.15$ meV do not destroy the soliton, while for $|E_n| \geq 0.20$ meV dispersion occurs. An additional mass disorder causes dispersion for $|E_n| \geq 0.10$ meV. For all parameters, increasing the disorder leads to dispersion of the traveling soliton and to the formation of a pinned excitation at the chain end when W and X are varied. Thus for the D_1 state the situation is reversed as compared to D_2. Here the soliton is rather stable against disorder in J_n, while it is extremely sensitive to disorder in W_n and X_n. Thus the formation of a soliton state in the quantum lattice is more difficult than in the classical lattice. This is also indicted by the higher threshold value of X for soliton formation.

IV. THE PARTIAL DRESSING MODEL

Brown and Ivic [34] have introduced a modified ansatz state which is called the $\tilde{D}$ state. The $\tilde{D}$ states are a subset of the D_1 states discussed above, where a fixed degree of phase mixing between phonons and excitons is incorporated [34]:

$$|\tilde{D}\rangle = \sum_n a'_n(t)\hat{a}'^{\dagger}_n \exp\left[\sum_k (b'_k \hat{b}'^{\dagger}_k - b'^{*}_k \hat{b}'_k)\right]|0\rangle \ . \quad (16)$$

Here the operators are given by

$$\hat{a}'_n = \hat{a}_n \exp\left[\delta \sum_k B_{nk}(\hat{b}'^{\dagger}_k - \hat{b}'_k)\right] \quad (17)$$

$$\hat{b}'_k = \hat{b}_k + \delta \sum_n B_{nk}\hat{a}^{\dagger}_n \hat{a}_n . \quad (18)$$

b is given in Appendix A and δ is the so-called dressing factor. The coefficients in the $\tilde{D}$ state are related to those in D_1 by

$$a_n = a'_n \exp\left[-i\delta \sum_k \mathrm{Im}(b'_k)\right] , \quad (19)$$

$$b_{nk} = -\delta B_{nk} + b'_k \ . \quad (20)$$

In (19) and (20) we used the fact that $\underline{B}$ is real or can be chosen as real via the phases of the normal modes. The total energy is given by

$$\begin{aligned} E_t = & \sum_n [E_0 + E_n - \delta(2-\delta) f_n]|a'_n|^2 \\ & + \sum_k \hbar\omega_k (|b'_k|^2 + \tfrac{1}{2}) \\ & - \sum_n a'^{*}_n (J_n a'_{n+1} + J_{n-1} a'_{n-1}) \\ & + 2(1-\delta) \sum_k \hbar\omega_k B_{nk}\, \mathrm{Re}(b'_k)|a'_n|^2 \end{aligned} \quad (21)$$

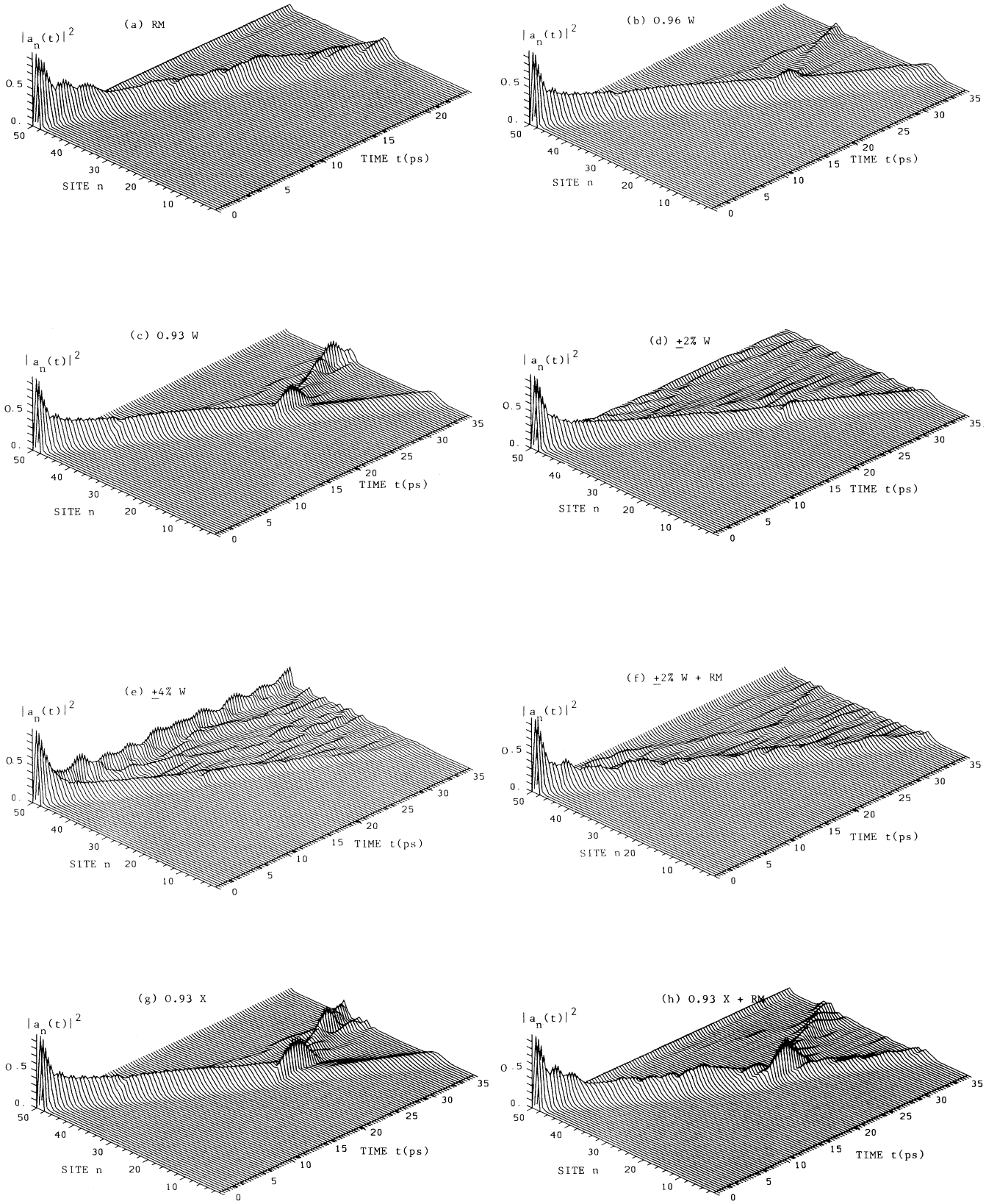

FIG. 7. Time evolution of $|a_n|^2$ for the D_1 state for some examples of disorder [$x\,A$ indicates an impurity in the middle of the chain where the parameter A is changed by a factor x; $\pm x\,\%\,A$ indicates random disorder within this range: $A_n=(1+\beta_n)A$, $|\beta_n|\leq x$, β_n random; RM indicates mass disorder].

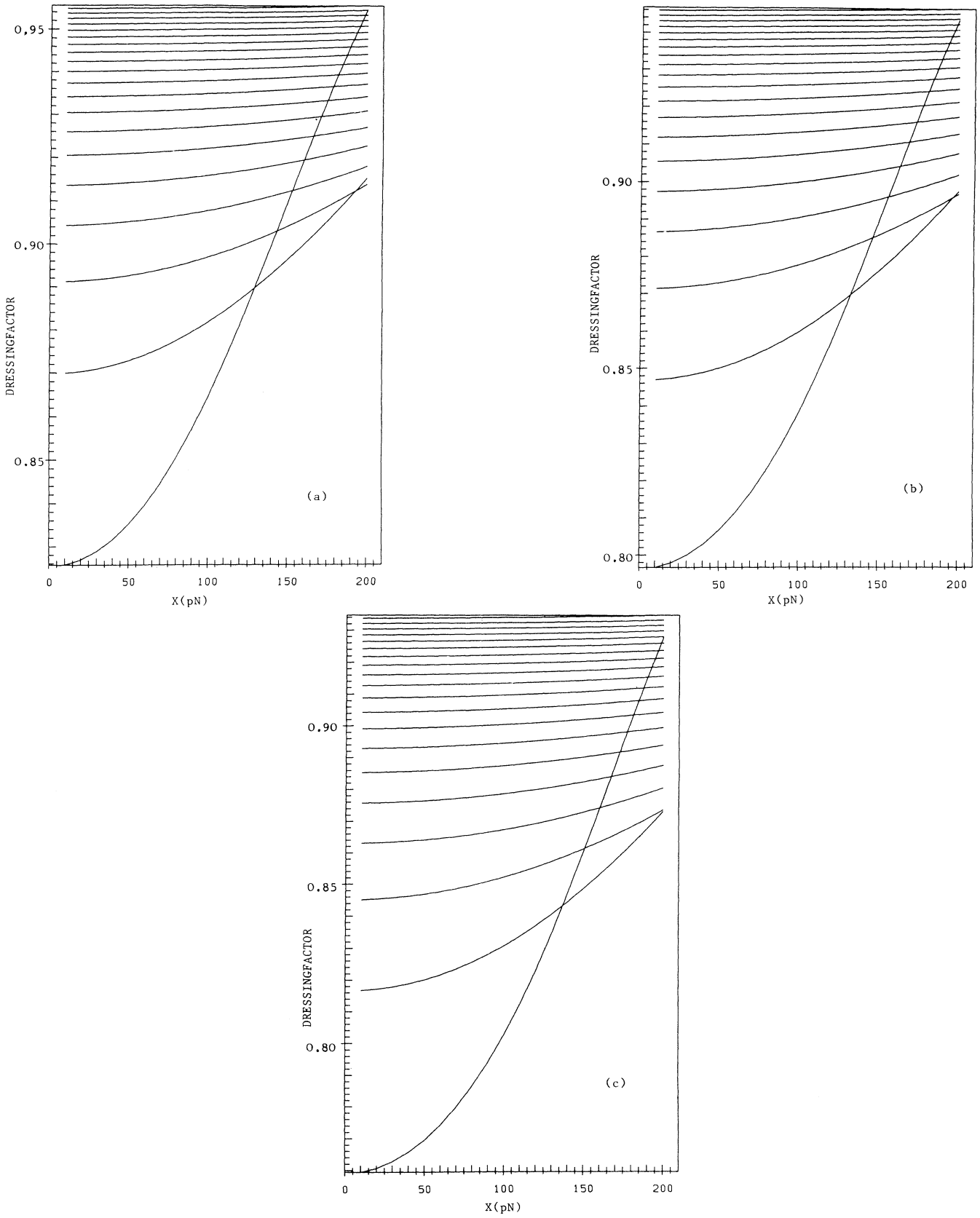

FIG. 8. The otpimized dressing factor δ as a function of X and W (lowest curve, $W=10$ N/m; upmost curve, $W=200$ N/m in steps of 10 N/m in between) for $J=0.8$ mev (a), 0.967 meV (b), and 1.2 meV (c).

f_n, the small polaron binding energy, is given by [34]

$$f_n = \sum_k B_{nk}^2 \hbar\omega_k \tag{22}$$

and the scaled oscillator coupling is

$$J_n' = J_n \exp\left[-\tfrac{1}{2}\delta^2 \sum_k (B_{nk} - B_{n+1,k})^2\right] . \tag{23}$$

The dressing factor δ can be obtained by minimalization of the averaged total energy [34]. Using Eqs. (4) and (12) of Ref. [34] we have computed δ for $T=0$ K in a periodic chain. The results are shown in Fig. 8. Comparison of the three figures shows that for 0.8 meV $\leq J \leq 1.2$ meV δ varies between 0.76 and 0.97, where δ decreases with increasing J. With increasing nonlinearity δ also increases; however, the larger W becomes, the smaller the variation in δ and the larger its value. Thus for increasing J and decreasing X and W the $\tilde{D}$ state approaches the D_2 state ($\delta=0$), while for decreasing J and increasing X and W $\tilde{D}$ approaches the small-polaron limit ($\delta=1$). For $J=0.967$

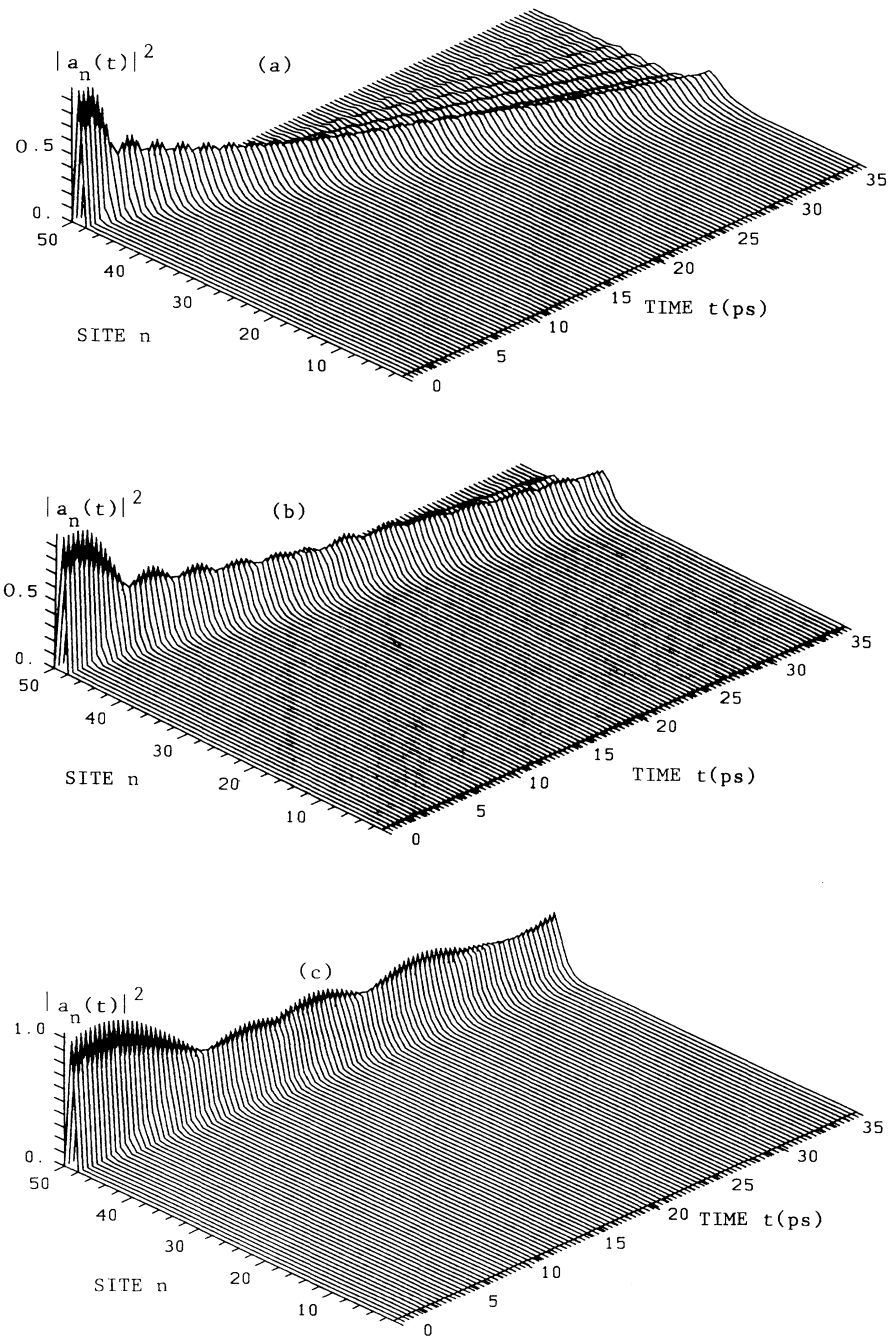

FIG. 9. Time evolution of $|a_n|^2$ for the $\tilde{D}$ state ($W=10$ N/m, $M=114m_n$, $J=0.967$ meV) $X=180$ pN (a), 220 pN (b), and 260 pN (c).

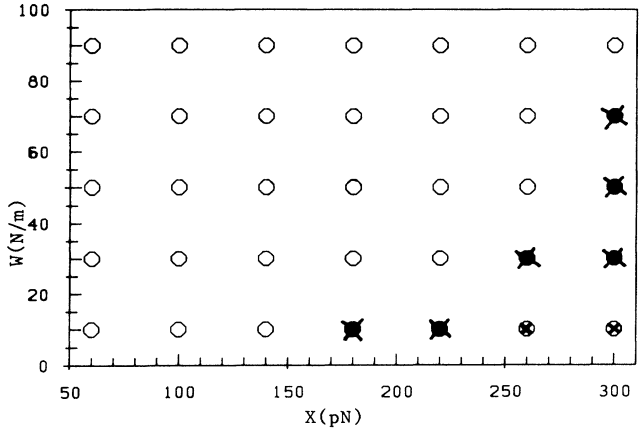

FIG. 10. Survey of the (X, W) parameter space as in Fig. 2 but for the $\tilde{D}$ state.

meV and $W=10$ N/m [Fig. 8(b), lowest curve] δ varies by ≈ 0.15 in the range $0 \leq X \leq 200$ pN. For $X=0$ $\delta \approx 0.796$ is obtained and for $X=200$ pN $\delta \approx 0.944$. For $X=60$ pN we obtain in agreement with Brown and Ivic [34] $\delta \approx 0.81$. Thus for the usually used values of the parameters the $\tilde{D}$ state is closer to the small-polaron limit than to the D_2 state [35].

Brown and Ivic [34] derived the equations of motion for the $\tilde{D}$ state with the help of the time-dependent variational principle. However, in their equations for a_n this variable also occurs on the right-hand side as an integrand. Thus numerical simulations would be difficult. However, this problem can be removed as shown in appendix C. In Fig. 9 we show the time evolution of $|a_n|^2$ for some typical cases as was previously shown for the D_1 state ($M=114m_p$, $W=10$ N/m, $J=0.967$ meV, $X=180$, 220, and 260 pN). First of all one notes that in contrast to D_2 and D_1 no real traveling soliton shows up. Only

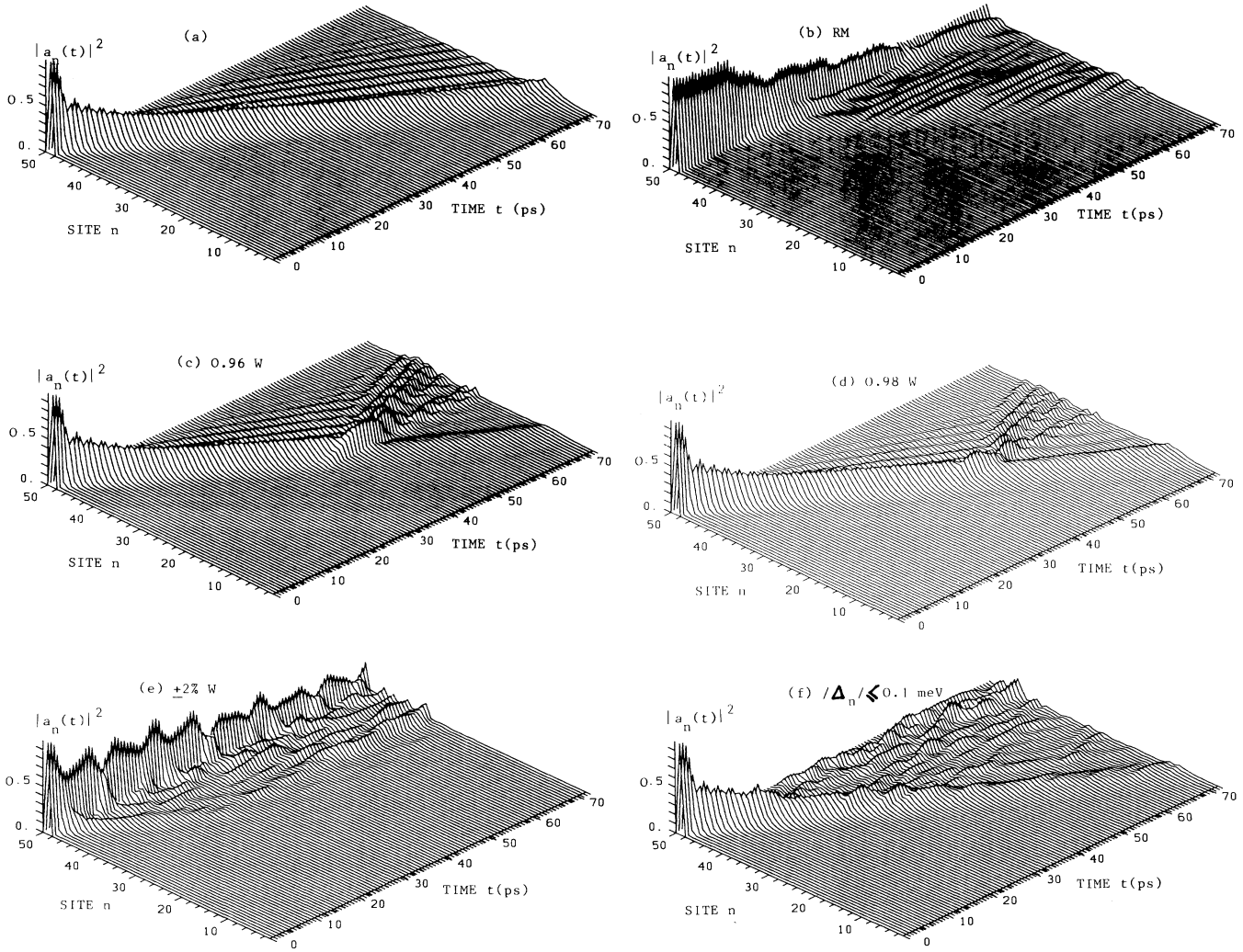

FIG. 11. Time evolution of $|a_n|^2$ in the $\tilde{D}$ state for some examples of disorder; the notation is the same as in Fig. 7 (in f) ($|\Delta_n| \leq x$ indicates random diagonal disorder within the range $\pm x$ for E_n).

from $X=180$ pN can one speak of a slowly dispersive solitary wave. For $X=260$ pN a pinned soliton is observed. In Fig. 10 we show our survey of the parameter space. Obviously for the $\tilde{D}$ state the parameter space which allows soliton formation is very small and at rather large values of X. Thus if the $\tilde{D}$ state would be a better approximation to the exact solution than D_2 or D_1, one would have to conclude that the Davydov soliton cannot exist in proteins already at $T=0$ K. However, the $\tilde{D}$ states are a subset of the D_1 states and the new D_1 equations [31,32] are derived with the time-dependent variational principle as well as the $\tilde{D}$ states [34]. Therefore the D_1 dynamics should be a better approximation to the exact ones than the $\tilde{D}$ dynamics. If the $\tilde{D}$ dynamics would approximate the exact solution better, then D_1 dynamics would numerically reduce to $\tilde{D}$ dynamics, which is not the case.

Turning to disorder effects, we show in Fig. 11(a) the dynamics of a periodic chain for $X=240$ pN ($W=13$ N/m, $J=0.967$ meV, $M=114m_p$). Figure 11(a) emphasizes again that within the $\tilde{D}$ states no real traveling soliton is present,and one has to deal with dispersive solitary waves or pinned solitons. Figure 11(b) shows the case of mass disorder and we have already seen that mass disorder destroys the solitary wave. For an impurity of strength $0.96W$ (or $1.04W$) in the middle of the chain the wave is fully reflected [Fig. 11(c)] and even for $0.98W$ (or $1.02W$) most of the wave is reflected [Fig. 11(a)]. Consequently for random disorder of strength $\pm 2\% W$ the wave is destroyed and most of the excitation remains at the chain end [Fig. 11(e)]. For an impurity of strength $0.98X$ (and $1.02X$) the wave is already reflected and random disorder of $\pm 2\% X$ leads to complete pinning. An impurity of $1.02X$ acts completely identically to one of $0.98X$. Thus the solitary waves in the $\tilde{D}$ state are even more sensitive to disorder in M, W, and X than the D_1 solitons. For impurities up to $0.96J$ we find no influence on the dynamics. The same holds for random disorder of $\pm 4\% J$. Thus we assume that for the parameter J the $\tilde{D}$ state behaves similar to the D_1 state. For a diagonal impurity of 0.3 meV roughly 50% of the excitation is reflected. A random diagonal disorder of ± 0.05 meV leads to enhanced dispersion but the wave still exists, while for ± 0.1 meV the wave disperses rapidly [Fig. 11(f)]. Thus, besides the fact that within the $\tilde{D}$ state no traveling solitons exist, the solitary waves are also more sensitive to disorder than in the other ansatz states discussed.

V. CONCLUSIONS

The basic conclusion from our calculations is that if the quantum character of the lattice is allowed to play a greater role than in the conventional D_2 state, traveling solitons occur at a much larger threshold values of X (D_1) or are not found at all ($\tilde{D}$). In a traveling soliton a lattice distortion has to follow the excitation in order to keep it localized, i.e., the lattice distortion is needed to stabilize the soliton against dispersion. However, a quantum system following a slow lattice distortion (e.g., an exciton in Davydov theory or the electrons in the Born-Oppenheimer approximation widely used in quantum chemistry) is characteristic for adiabatic approximations. Therefore in D_2 theory (adiabatic, classical lattice) soliton formation occurs more easily than in D_1 theory (quantum lattice). If the quantum nature of the lattice were negligible, thus justifying an adiabatic approximation, D_1 dynamics would be numerically similar to D_2 dynamics. That this is not the case shows that for the Davydov Hamiltonian an adiabatic description is not appropriate. Only for large values of X and W is the lattice able to follow and thus stabilize a soliton. However, as will be shown in later papers [36,37] inclusion of temperature shifts the stability region for solitons to parameter values reasonable for proteins.

Further in D_1 states the soliton is very sensitive to disorder in parameter sequences along the chain that directly influence the lattice (W,X), while it is more robust against disorder in the oscillator system (J). In the D_2 state the situation is reversed. This is due to the fact that in $|D_1\rangle$ theory a factor $D_{n,n\pm 1}$ appears in the terms including J. This exponential factor effectively reduces J and thus also the effects of disorder in J. However in D_2 the absolute values of disorder in E_n against which the soliton is stable are of the same order of magnitude as in D_1. Thus one has to conclude that solitons are more sensitive to disorder in quantum systems (oscillators in D_1 and D_2; oscillators and lattice in D_1) than in classical systems (lattice in D_2). However the large threshold value of X in D_1 (160–180 pN) implies that if D_1 is approximately correct, the Davydov mechanism—coupling of C=O stretch to hydrogen bonds—cannot function at $T=0$ K, since in proteins $X=30$–62 pN is estimated. Moreover proteins are aperiodic by their very nature, hence the sensitivity of the solitons to disorder points also against the standard Davydov mechanism.

The equations of motion used for all ansatz states considered ($D_1,D_2,\tilde{D}$) are obtained with the same quantum-mechanical method, namely, the time-dependent variational principle. The same equations can also be obtained by other quantum-mechanical methods [31,32,34], but in the case of D_1 and $\tilde{D}$ not by the standard Davydov method [28,29], which is correct only for D_2 [26]. Both $D_2(b_{nk}=b_k)$ and $\tilde{D}(b_{nk}=-\delta B_{nk}+b_k)$ are subsets of the most general $D_1(b_{nk})$ states. Thus D_1 must be the best approximation to the actual dynamics among these ansatz states. If D_2 or $\tilde{D}$ would be the best approximation, D_1 dynamics would reduce to D_2 or $\tilde{D}$ dynamics at least numerically. However, it is known that although for D_1 [32]

$$\left\langle D_1 \left| \hat{H} - i\hbar \frac{\partial}{\partial t} \right| D_1 \right\rangle = 0 \tag{24}$$

holds, D_1 is exact only for the transportless case ($J=0$). In all other cases one has

$$\left[\hat{H} - i\hbar \frac{\partial}{\partial t} \right] |D_1\rangle = |\beta\rangle \neq 0 \quad \text{if } J \neq 0 \tag{25}$$

where $\langle D_1|\beta\rangle = 0$. Thus one would need a method that would allow to study the error $|\beta\rangle$ numerically. It may still be possible that the exact dynamics contain more stable solitons than D_1. Further, temperature effects in

D_1 shift the stability region of solitons to parameter values that are reasonable for proteins [36,37]. Finally, it should be kept in mind that instead of the C=O stretch also the N—H vibration is coupled to the hydrogen bonds with a much larger coupling constant (roughly 300 pN).

In addition neither accurate parameter values nor the degree of disorder in the parameters for proteins are known. Since exact measurements on biopolymers are extremely difficult this problem could possibly be solved by theory and work on this is already published (see, e.g., [33]). Thus the question of whether or not the Davydov mechanism for energy transport and storage can function in proteins is still a completely open one and a great deal of further experimental and theoretical work is necessary to reach a final answer.

ACKNOWLEDGMENTS

The financial support of the Deutsche Forschungsgemeinschaft, Project No. 0t 51/6-2) and of the Fonds der chemischen Industrie is gratefully acknowledged.

APPENDIX A: THE DISORDERED HAMILTONIAN

We start with the classical equations of motion for a chain of N harmonically coupled point masses (M_n):

$$\underline{M}\ddot{\mathbf{q}}=-\underline{W}\mathbf{q},\quad M_{nm}=M_n\delta_{nm}\ ,$$
$$W_{nm}=[W_n(1-\delta_{nN})+W_{n-1}(1-\delta_{n1})]\delta_{nm} - W_n(1-\delta_{nN})\delta_{m,n+1}-W_{n-1}(1-\delta_{n1})\delta_{m,n-1}\ , \tag{A1}$$

where q_n is the displacement of the unit n and W_n the harmonic force constant between units n and $n+1$. $p_n=M_n\dot{q}_n$ are the momenta of the units. Using the transformation

$$\underline{V}=\underline{M}^{-1/2}\underline{W}\,\underline{M}^{-1/2},\quad \mathbf{d}=\underline{M}^{1/2}\mathbf{q},\quad \mathbf{p}=\underline{M}^{1/2}\dot{\mathbf{d}} \tag{A2}$$

we obtain

$$\ddot{\mathbf{d}}=-\underline{V}\mathbf{d}\ . \tag{A3}$$

The Hamilton function is transformed as

$$2H_{\rm ph}=\mathbf{p}^{\dagger}\underline{M}^{-1}\mathbf{p}+\mathbf{q}^{\dagger}\underline{W}\mathbf{q}=\dot{\mathbf{d}}^{\dagger}\dot{\mathbf{d}}+\mathbf{d}^{\dagger}\underline{V}\mathbf{d}\ . \tag{A4}$$

(A3) can be further simplified by transformation to normal modes $\mathbf{U}_k$ with

$$\mathbf{d}=\sum_k \mathbf{U}_k[\underline{U}^{\dagger}\mathbf{d}(0)]_k\exp(i\omega_k t)$$

such that

$$\underline{U}^{\dagger}\underline{V}\,\underline{U}=\underline{\omega}^2,\quad \omega_{kl}^2=\omega_k^2\delta_{kl}\ . \tag{A5}$$

$\underline{V}$ can be numerically diagonalized to obtain the normal modes $\underline{U}$ which can be chosen to be real. With $\mathbf{b}=\underline{U}^{\dagger}\mathbf{d}$ we obtain

$$2H_{\rm ph}=\dot{\mathbf{b}}^{\dagger}\dot{\mathbf{b}}+\mathbf{b}^{\dagger}\underline{\omega}^2\mathbf{b}\ , \tag{A6}$$

and with $\mathbf{b}=\hbar\underline{\omega}^{-1/2}\mathbf{a}$, $\mathbf{c}=\omega^{-1}\dot{\mathbf{a}}$, $H_{\rm ph}$ becomes

$$2H_{\rm ph}=\sum_k \hbar\omega_k(c_k^*c_k+a_k^*a_k)\ . \tag{A7}$$

Now creation ($\hat{b}_k^{\dagger}$) and annihilation ($\hat{b}_k$) operators are introduced in the usual way to obtain the phonon part of the Hamilton operator:

$$a_k\rightarrow\frac{1}{\sqrt{2}}(\hat{b}_k+\hat{b}_k^{\dagger}),\quad c_k\rightarrow-\frac{i}{\sqrt{2}}(\hat{b}_k-\hat{b}_k^{\dagger}) \tag{A8}$$

which leads to

$$\hat{H}_{\rm ph}=\sum_k \hbar\omega_k(\hat{b}_k^{\dagger}\hat{b}_k+\tfrac{1}{2}) \tag{A9}$$

and thus

$$\hat{q}_n=\sum_k\left[\frac{\hbar}{2M_n\omega_k}\right]^{1/2}U_{nk}(\hat{b}_k^{\dagger}+\hat{b}_k)\ ,$$
$$\hat{p}_n=i\sum_k(\tfrac{1}{2}\hbar M_n\omega_k)^{1/2}U_{nk}(\hat{b}_k^{\dagger}-\hat{b}_k)\ . \tag{A10}$$

Introducing (A10) into the full Hamiltonian we obtain finally

$$\hat{H}=\sum_n[(E_0+E_n)a_n^{\dagger}a_n-J_n(\hat{a}_n^{\dagger}\hat{a}_{n+1}+\hat{a}_{n+1}^{\dagger}\hat{a}_n)] +\sum_k\hbar\omega_k(\hat{b}_k^{\dagger}\hat{b}_k+\tfrac{1}{2})+\sum_{n,k}\hbar\omega_k B_{nk}(\hat{b}_k^{\dagger}+\hat{b}_k)\hat{a}_n^{\dagger}\hat{a}_n\ . \tag{A11}$$

Note that the creation ($\hat{a}_n^{\dagger}$) and annihilation ($\hat{a}_n$) operators for vibrational quanta at site n and the quantities a_k in Eqs. (A7) and (A8) are not related to each other. $\underline{B}$ is given by

$$B_{nk}=\frac{X_n}{\omega_k}\left[\frac{1}{2\hbar\omega_k}\right]^{1/2}\left[\frac{U_{n+1,k}}{\sqrt{M_{n+1}}}-\frac{U_{nk}}{\sqrt{M_n}}\right]\ . \tag{A12}$$

APPENDIX B: TEMPERATURE IN D_1 THEORY

To include temperature into the model one can use the thermally averaged Hamiltonian H_T of Ref. [39] together with the Euler-Lagrange equations derived in Ref. [32]:

$$i\hbar\dot{a}_n+\frac{i\hbar}{2}a_n\sum_k(\dot{b}_{nk}b_{nk}^*-\dot{b}_{nk}^*b_{nk})=\frac{\partial H_T}{\partial a_n^*}\ , \tag{B1}$$

$$\frac{i\hbar}{2}|a_n|^2\dot{b}_{nk}+\frac{i\hbar}{2}\frac{d}{dt}(|a_n|^2b_{nk})=\frac{\partial H_T}{\partial b_{nk}^*}\ , \tag{B2}$$

and H_T of Ref. [29] generalized to the disorder case is given by

$$H_T=\sum_n\Big\{(E_0+E_n)|a_n|^2 -J_nD_{n,n+1}a_n^*a_{n+1}-J_{n-1}D_{n,n-1}a_n^*a_{n-1} +|a_n|^2\sum_k\hbar\omega_k[B_{nk}(b_{nk}+b_{nk}^*)+V_k+|b_{nk}|^2]\Big\}\ , \tag{B3}$$

where

$$V_k = \left[\exp\left[\frac{\hbar\omega_k}{k_B T}\right]-1\right]^{-1} \tag{B4}$$

and

$$D_{n,n\pm1}=\exp\left[\sum_k[(V_k+1)b_{nk}^* b_{n\pm1,k}+V_k b_{nk} b_{n\pm1,k}^* - (V_k+\tfrac{1}{2})(|b_{nk}|^2+|b_{n\pm1,k}|^2)]\right] . \tag{B5}$$

Together with $\partial H_T/\partial a_n^*$ from [29] we obtain

$$i\hbar\dot{a}_n = \left[-\frac{i\hbar}{2}\sum_k(\dot{b}_{nk}b_{nk}^*-\dot{b}_{nk}^* b_{nk})+E_n\right]a_n - J_{n-1}D_{n,n-1}a_{n-1}-J_n D_{n,n+1}a_{n+1} + a_n\sum_k \hbar\omega_k[B_{nk}(b_{nk}+b_{nk}^*)+|b_{nk}|^2] . \tag{B6}$$

Here the gauge transformation

$$a_n = a_n' \exp\left[-i\left[E_0+\sum_k \hbar\omega_k V_k\right]t/\hbar\right] \tag{B7}$$

was used and a_n' was replaced by a_n again afterwards in (B6). Using (B2) one obtains

$$i\hbar|a_n|^2\dot{b}_{nk} = \frac{\partial H_T}{\partial b_{nk}^*} - \frac{i\hbar}{2}b_{nk}(\dot{a}_n^* a_n+\dot{a}_n a_n^*) . \tag{B8}$$

Together with (B6) one obtains

$$\frac{i\hbar}{2}b_{nk}(\dot{a}_n^* a_n+\dot{a}_n a_n^*) = \tfrac{1}{2}b_{nk}J_n(a_n a_{n+1}^* D_{n+1,n}-a_n^* a_{n+1}D_{n,n+1}) + \tfrac{1}{2}b_{nk}J_{n-1}(a_n a_{n-1}^* D_{n-1,n}-a_n^* a_{n-1}D_{n,n-1}) . \tag{B9}$$

With $\partial H_T/\partial b_{nk}^*$ from [29] we obtain finally

$$i\hbar\dot{b}_{nk} = \hbar\omega_k(B_{nk}+b_{nk})-J_{n-1}(b_{n-1,k}-b_{nk})\left[(V_k+1)D_{n,n-1}\frac{a_{n-1}}{a_n}+V_k D_{n-1,n}\frac{a_{n-1}^*}{a_n^*}\right] - J_n(b_{n+1,k}-b_{nk})\left[(V_k+1)D_{n,n+1}\frac{a_{n+1}}{a_n}+V_k D_{n+1,n}\frac{a_{n+1}^*}{a_n^*}\right] . \tag{B10}$$

Applications of these optimized D_1 equations including temperature and disorder are in progress [36,37]. Note that the thermal average performed to obtain H_T is equivalent to the computation of dynamics for all states populated with fixed phonon distribution and a subsequent thermal average of these results.

APPENDIX C: IMPLEMENTATION OF $\tilde{D}$ DYNAMICS

The term which leads to technical difficulties appears in the equation for $b_k'(t)$ in [34]:

$$\int_0^t \exp[i\omega_k(t-t')]\sum_n B_{nk}\frac{d}{dt'}|a_n'(t')|dt' . \tag{C1}$$

Integration by parts yields

$$-i\omega_k\int_0^t \exp[i\omega_k(t-t')]\sum_n B_{nk}|a_n'(t')|^2dt' + \sum_n B_{nk}|a_n'(t)|^2-\exp(-i\omega_k t)\sum_n B_{nk}|a_n'(0)|^2 . \tag{C2}$$

Thus $b_k'(t)$ is finally given by

$$b_k'(t)= \left[b_k'(0)-\delta\sum_n B_{nk}|a_n'(0)|^2\right]\exp(-i\omega_k t) +\delta\sum_n B_{nk}|a_n'(t)|^2 -i\omega_k\int_0^t \exp[i\omega_k(t-t')]\sum_n B_{nk}|a_n'(t')|^2dt' . \tag{C3}$$

For numerical simulations a suitably small time step t_0 is introduced. During this time step (or half of it as in the Runge-Kutta method) the integrand is linearly interpolated. Thus at time lt_0 we obtain

$$\begin{aligned} b_k'(l) &= A_k\exp(-i\omega_k lt_0)+C_k(l) -i\omega_k\exp(-i\omega_k lt_0)\sum_n B_{nk}D_{nk}(l) ,\\ A_k &= b_k'(0)-\delta\sum_n B_{nk}|a_n'(0)|^2 ,\\ C_k(l) &= \delta\sum_n B_{nk}|a_n'(l)|^2 ,\\ D_{nk}(l) &= D_{nk}(l-1)+(t_0/2)[E_{nk}(l)+E_{nk}(l-1)] ,\\ D_{nk}(0) &= 0 ,\\ E_{nk}(l) &= \exp(i\omega_k lt_0)|a_n'(l)|^2 \end{aligned} \tag{C4}$$

For $T=0$ K the initial phonon data are $b_k'(0)=0$. After computation of $a_n'(l)$ and $b_k'(l)$ at time lt_0 the time derivative of $a_n'(l)$ can be calculated;

$$i\hbar\dot{a}_n'(l)=[E_0+E_n-\delta(2-\delta)f_n]a_n'(l) -J_n'a_{n+1}'(l)-J_{n-1}'a_{n-1}'(l) +2\sum_k \hbar\omega_k B_{nk}\,\mathrm{Re}[b_k'(l)]a_n'(l) +2\delta(1-\delta)\sum_{m,k}\hbar\omega_k B_{nk}B_{mk}|a_m'(l)|^2 a_n'(l) . \tag{C5}$$

From $\dot{a}_n'(l)$ then $a_n'(l+1)$ can be computed and then $b_k'(l+1)$. In practice, as usual, a gauge transformation is performed,

$$a_n''=a_n' \exp(iE_0 t/\hbar) , \tag{C6}$$

which removes the term containing E_0 from (C5) and thus the fast oscillating part of a_n'. Finally from $b_{nk}=-\delta B_{nk}+b_k'$ the momenta p_n and displacements q_n of the lattice units can be obtained:

$$p_n(l)=\sum_{k,m}(2\hbar M_n\omega_k)^{1/2}U_{nk}|a_m(l)|^2\,\mathrm{Im}[b_{mk}(l)] , \tag{C7}$$

$$q_n(l)=\sum_{k,m}(2\hbar/M_n\omega_k)^{1/2}U_{nk}|a_m(l)|^2\,\mathrm{Re}[b_{mk}(l)] . \tag{C8}$$

Typically a time step of $t_0=5$ fs was used in our simulations within a Runge-Kutta method correct up to fourth order. In typical cases ($M=114m$, $W=13$ N/m, $J=0.967$ meV, $X=240$ pN) for a periodic chain of 50 units within 70 ps the error in total energy was less than 50 μeV ($\approx 0.02\% E_t$) and the norm is conserved to better than 4×10^{-4}. In this case $\delta=0.9016$ and the translational mode was kept unpopulated.

As already discussed in the paper by Brown and Ivic [34] the inclusion of temperature enters in the determination of δ, where a thermal average is involved, via the quantity

$$S_n(T)=\tfrac{1}{2}\sum_k (B_{nk}-B_{n+1,k})^2 \coth\left[\frac{\hbar\omega_k}{2k_BT}\right] \tag{C9}$$

and thus in J_n' in the form of a Debye-Waller factor

$$J_n'(T)=J_n \exp[-\delta^2 S_n(T)] . \tag{C10}$$

Further in the equations of motion temperature appears directly in the phonon initial data $b_k'(0)$. These can be approximately obtained in the same way as for D_2 dynamics. One can populate all modes (except the translational one) of the lattice corresponding to a Bose-Einstein distribution and solve the dynamical problem of the decoupled lattice [35]. With p_n and q_n at some arbitrary time t' (the results do not depend on t' as shown previously [18], one can calculate

$$\mathrm{Re}[b_k'(0)]=\sum_n (M_n\omega_k/2\hbar)^{1/2}U_{nk}q_n(t') , \tag{C11}$$

$$\mathrm{Im}[b_k'(0)]=\sum_n (\tfrac{1}{2}\hbar M_n\omega_k)^{1/2}U_{nk}p_n(t') \tag{C12}$$

and use these values as input for the time simulation. Calculations along this line are in progress. As in the case of D_1 dynamics one has to note that the larger X is, the smaller the time step has to be chosen.

[1] E. Fermi, J. R. Pasta, and S. M. Ulam, Los Alamos Laboratory Report No. La-1940 (1955).

[2] J. Scott-Russel, Proc. R. Soc. Edinburg, p. 319 (1844).

[3] H. J. Mikeska, J. Phys. C **11**, L29 (1978).

[4] K. Maki, J. Low Temp. **41**, 327 (1980).

[5] K. J. Wahlstrand, J. Chem. Phys. **82**, 5247 (1985); K. J. Wahlstrand and P. G. Woylness, *ibid.* **82**, 3392 (1976).

[6] S. Aubry, J. Chem. Phys. **64**, 3392 (1976).

[7] M. A. Collins, A. Blumen, J. F. Curtis, and J. Ross, Phys. Rev. B **19**, 3630 (1979).

[8] J. A. Krumhansl and D. M. Alexander, in *Structure and Dynamics: Nucleic Acids and Proteins,* edited by E. Clementi and R. H. Sarma (Adenine, New York, 1983), p. 61.

[9] J. Ladik and J. Čížek, Int. J. Quantum Chem. **26**, 955 (1984); J. Ladik, in *Molecular Basis of Cancer, Part A,* edited by R. Rein (Alan Liss Co., New York, 1985), p. 343; D. Hofmann, W. Förner, and J. Ladik, Phys. Rev. A **37**, 4429 (1988); W. Förner, *ibid.* **38**, 939 (1988); **40**, 6435 (1989); W. Förner, P. Otto, J. Ladik, and F. Martino, *ibid.* **40**, 6457 (1989); D. Hofmann, W. Förner, and J. Ladik, J. Phys. Condens. Matter **2**, 4081 (1990).

[10] W. P. Su, J. R. Schrieffer, and A. J. Heeger, Phys. Rev. Lett. **42**, 1698 (1979); W. P. Su, Solid State Commun. **35**, 899 (1980); W.P. Su, J. R. Schrieffer, and A. J. Heeger, Phys. Rev. B **22**, 2099 (1980); W. P. Su and J. R. Schrieffer, Proc. Natl. Acad. Sci. (U.S.A.) **77**, 5626 (1980); F. Guinea, Phys. Rev. B **30**, 1884 (1984); A. R. Bishop, D. K. Campbell, R. P. Lomdahl, L. Horovitz, and S. R. Phillpot, Phys. Rev. Lett. **52**, 671 (1984); W. Förner, M. Seel, and J. Ladik, Solid State Commun. **57**, 463 (1986); J. Chem. Phys. **84**, 5910 (1986); A. Godzik, M. Seel, W. Förner, and J. Ladik, Solid State Commun. **60**, 609 (1987); C.-M. Liegener, W. Förner, and J. Ladik, *ibid.* **61**, 203 (1987); S.R. Phillpot, FD. Beariswyl, A. R. Bishop, and P. S. Lomdahl, Phys. Rev. B **35**, 7533 (1987); S. Kivelson and D. E. Heim, *ibid.* **26**, 4278 (1982); A. J. Heeger and J. R. Schrieffer, Solid State Commun. **48**, 207 (1983); Z. Soos and S. Ramasesha, Phys. Rev. Lett. **51**, 2374 (1983); M. Sasai and H. Fukutome, Synth. Metals **9**, 295 (1984); W. P. Su, Phys. Rev. B **34**, 2988 (1986); S. Kivelson and Wei-Kang Wu, *ibid.* **34**, 5423 (1986); C.-L. Wang and F. Martino, *ibid.* **34**, 5540 (1986); W. Förner, C. L. Wang, F. Martino, and J. Ladik, *ibid.* **37**, 4567 (1988); W. Förner, Solid State Commun. **63**, 941 (1987); R. Markus, W. Förner, and J. Ladik, *ibid.* **68**, 135 (1988); H. Orendi, W. Förner, and J. Ladik, Chem. Phys. Lett. **150**, 113 (1988).

[11] A. Szent-Györgyi, Nature **148**, 157 (1941); Science **93**, 609 (1941); A. K. Bakhshi, P. Otto, J. Ladik, and M. Seel, Chem. Phys. **20**, 683 (1986).

[12] A. S. Davydov and N. I. Kislukha, Phys. Status Solidi B **59**, 465 (1973); A. S. Davydov, Phys. Scr. **20**, 387 (1979); A. S. Davydov, Usp. Fiz. Nauk **138**, 603 (1982) [Sov. Phys.—Usp. **25**, 898 (1982)]; A. S. Davydov, *Biology and Quantum Mechanics* (Pergamon, Oxford, 1982).

[13] G. Careri, U. Buontempo, F. Galuzzi, A. C. Scott, E. Gratton, and E. Shyamsunder, Phys. Rev. B **30**, 4689 (1984); J. C. Eilbeck, P. S. Lomdahl, and A. C. Scott, *ibid.* **30**, 4703 (1984).

[14] W. Fann, L. Rothberrg, M. Roberson, S. Benson, J. Madey, S. Etemad, and R. Austin, Phys. Rev. Lett. **64**, 607 (1990).

[15] J. Halding and P. S. Lomdahl, Phys. Lett. A **124**, 37 (1987).

[16] Q. Li, St. Pnevmatikos, E. N. Economu, and C. M. Soukoulis, Phys. Rev. B **37**, 3534 (1988).
[17] H. Motschmann, W. Förner, and J. Ladik, J. Phys. Condens. Matter **1**, 5083 (1989).
[18] W. Förner and J. Ladik, in *Davydov's Soliton Revisited: Self Trapping of Vibrational Energy in Proteins,* Vol. 243 of NATO Advanced Study Institute, Series B: Physics, edited by P. L. Christiansen and A. C. Scott (Plenum, New York, 1991), p. 267.
[19] W. Förner, J. Phys. Condens. Matter **3**, 3235 (1991).
[20] D.Hofmann, W. Förner, and J. Ladik, J. Phys. C **2**, 4081 (1990).
[21] A. C. Scott, Phys. Rev. A **26**, 578 (1982); in *Structure and Dynamics: Nucleic Acids and Proteins,* edited by E. Clementi and R. H. Sarma (Adenine, New York, 1983), pp. 389; Phys. Scr. **29**, 279 (1984); L. MacNeil and A. C. Scott, *ibid.* **29**, 284 (1984); A. C. Scott, Philos. Trans. R. Soc. London A **315**, 423 (1985).
[22] J. M. Ziman, Elements of Advanced Quantum Theory (Cambridge University Press, Cambridge, 1969).
[23] N. A. Nevskaya and Y. N. Chirgadze, Biopolymers **15**, 637 (1976).
[24] A. Novak, *Structure and Bonding* (Springer, Berlin, 1974), Vol. 18.
[25] V. A. Kuprievich and V. W. Klymenko, Mol. Phys. **34**, 1287 (1977).
[26] W. C. Kerr and P. S. Lomdahl, Phys. Rev. B **35**, 3629 (1987).
[27] J. Stiefel, *Einführung in die Numerische Mathematik* (Teubner Verlag, Stuttgart, 1965).
[28] A. S. Davydov, Zh. Eksp. Teor. Fiz. **78**, 789 (1980) [Sov. Phys.—JETP **51**, 397 (1980)].
[29] L. Cruzeiro, J. Halding, P. L. Christiansen, O. Skovgaard, and A. C. Scott, Phys. Rev. A **37**, 880 (1988).
[30] D. W. Brown, K. Lindenberg, and B. J. West, Phys. Rev. A **33**, 4104 (1986); D. W. Brown, *ibid.* **37**, 5010 (1988); D. W. Brown, K. Lindenberg, and B. J. West, *ibid.* **35**, 6169 (1987); **37**, 2946 (1988).
[31] B. Mechtly and P. B. Shaw, Phys. Rev. B **38**, 3075 (1988).
[32] M. J. Skrinjar, D. V. Kapor, and S. D. Stojanovic, Phys. Rev. A **38**, 6402 (1988); Phys. Rev. B **40**, 1984 (1989).
[33] B. M. Bierce, in *Proceedings of the MIDIT 1989 Workshop, Hanstholm, 1989* (Plenum, New York, in press).
[34] D. W. Brown and Z. Ivic, Phys. Rev. B **40**, 9876 (1989).
[35] Note that in [34] cyclic boundary conditions and the symmetric interaction Hamiltonian were used. Further δ depends on chain length. We could reproduce the δ value for $T=0$ K given in [34] (cyclic chain, symmetric interaction, numerical calculation of eigenvectors and eigenfrequencies) for a chain of 1000 sites to an accuracy of three digits. However, for $T=300$ K we find $\delta=0.43$ while in [34] $\delta=0.68$ is given. In the case of disorder we take the average values of site-dependent quantities appearing in the determination of δ.
[36] W. Förner (unpublished).
[37] W. Förner, in proceedings of the Workshop on Coherent and Emergent Phenomena in Biomolecular Systems, Tucson, Arizona, 1991, edited by S. Hamerott, S. Rasmussen, and A. C. Scott [Nanobiology (to be published)].